

Supporting Information (SI) for:

Multi-Site Orbital Coupling in Ru-based High-Entropy Alloy Enabled Hydroxyl Spillover for Boosted Peroxidase-like Activity

Qi Yang^{ab†}, Jiawei Zhang^{a†}, Yuxi Tang^a, Yan Ju^a, Xuejiao Gao^{c}, Chaoyang Chu^d, Huimin Jia^{ab*}, Weiwei He^{ab*}*

^aKey Laboratory of Micro-Nano Materials for Energy Storage and Conversion of Henan Province, Institute of Surface Micro and Nano Materials, College of Chemical and Materials Engineering, Xuchang University, Xuchang, Henan 461000, P. R. China

^bHenan Joint International Research Laboratory of Nanomaterials for Energy and Catalysis, Xuchang University, Xuchang, Henan 461000, China

^cCollege of Chemistry and Chemical Engineering, Jiangxi Normal University, Nanchang 330022, P. R. China

^dShanghai Key Laboratory of High-resolution Electron Microscopy, School of Physical Science and Technology, ShanghaiTech University.

*** Corresponding author E-mail:**

gaoxj@jxnu.edu.cn (Xuejiao Gao), jhmxcu2015@163.com (Huimin Jia),

heweiveixcu@gmail.com (Weiwei He)

Notes

The authors declare no competing financial interest.

EXPERIMENTAL SECTION

Density Functional Theory Calculations

Geometry optimizations and total energy estimations utilized the generalized gradient approximation (GGA), particularly the Perdew-Burke-Ernzerhof (PBE) functional, which was enhanced by the addition of van der Waals interactions using the DFT-D3BJ method.¹⁻³ A rigorous energy cut-off was established at 500 eV, while Gaussian smearing was applied at 0.05 eV to improve the precision of the computational processes. The integration over the Brillouin zone was precisely carried out using a (3×3×1) Monkhorst-Pack k-point grid.⁴ The accuracy of the computations was maintained by setting stringent convergence thresholds for the electronic structure and ionic forces, specifically at 10^{-5} eV and 0.02 eV Å⁻¹, respectively. These calculations were performed using the Vienna Ab initio Simulation Package (VASP), which employs the projector-augmented wave (PAW) method for the generation of pseudopotentials.⁵⁻⁷

RESULTS AND DISCUSSION

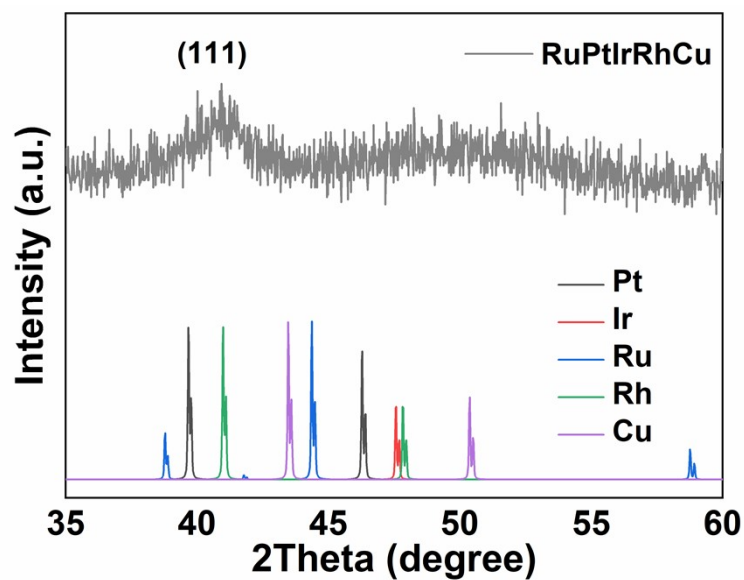


Figure S1. XRD pattern of RuPtIrRhCu HEAzymes containing the standard diagram of Pt, Ir, Ru, Rh, Cu.

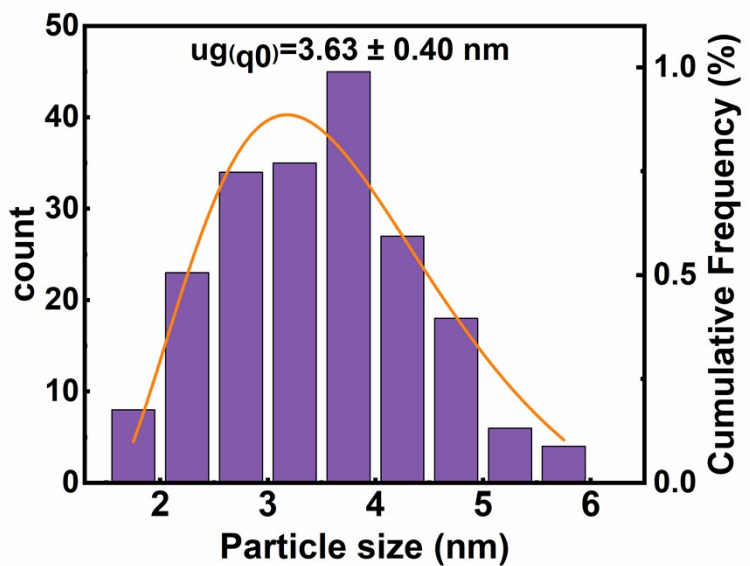


Figure S2. Size distribution of RuPtIrRhCu HEAzymes.

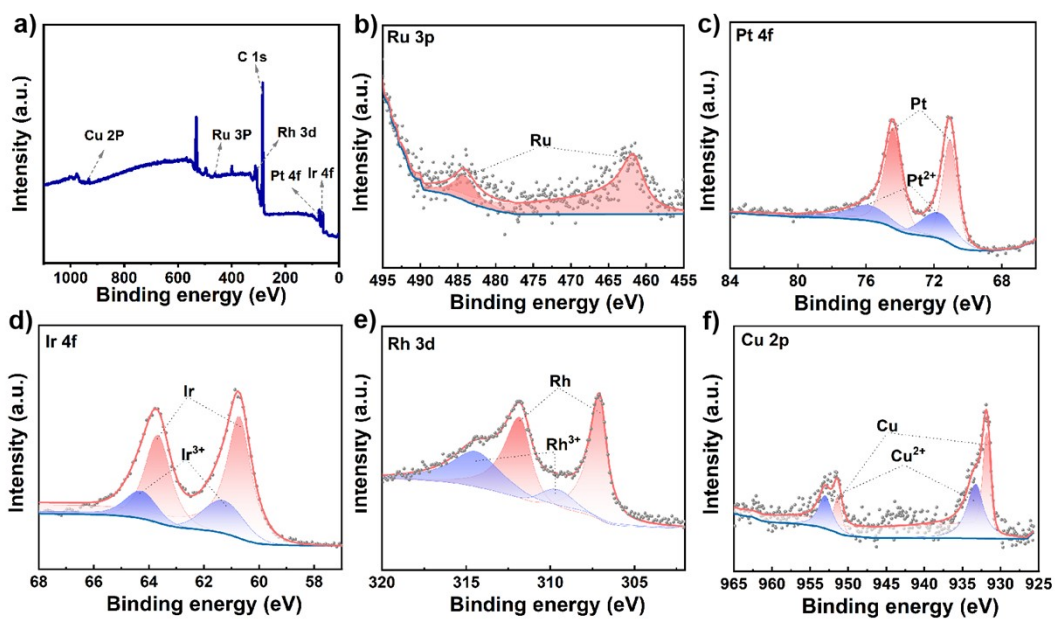


Figure S3. Typical XPS survey of (a) RuPtIrRhCu HEAzymes, (b) Ru 3p, (c) Pt 4f, (d) Ir 4f, (e) Rh 3d, (e) Cu 2p.

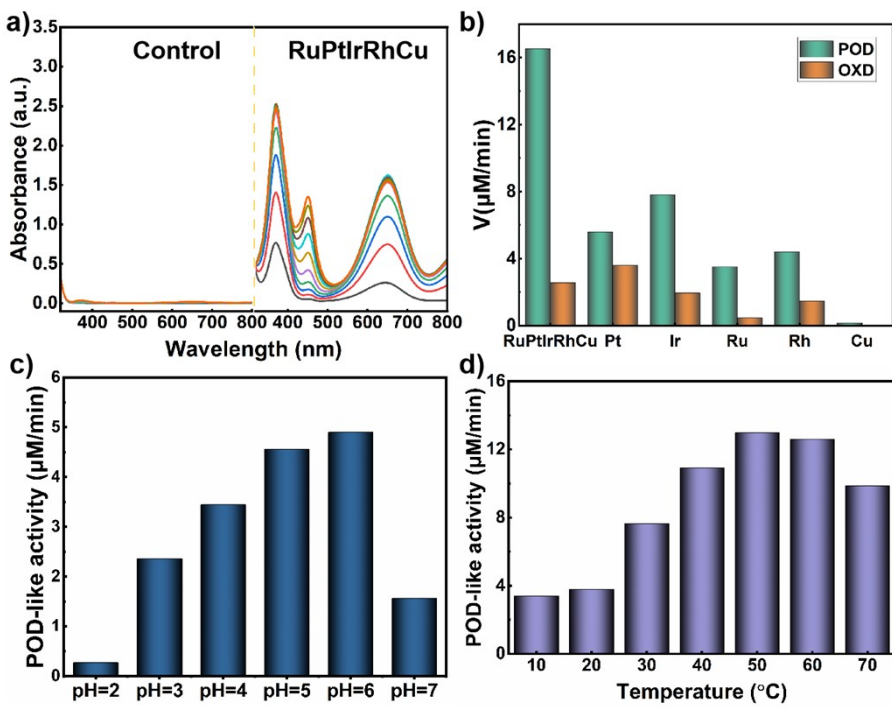


Figure S4. (a) UV-Vis absorption spectra of TMB catalyzed oxidation with or without HEAzymes. (b) Histogram of POD- and OXD-like activity of HEAzymes and single metal NPs at 25 °C. (c) Histogram of POD-like activity of HEAzymes at different pH. (d) Histogram of POD-like activity of HEAzymes at different temperatures.

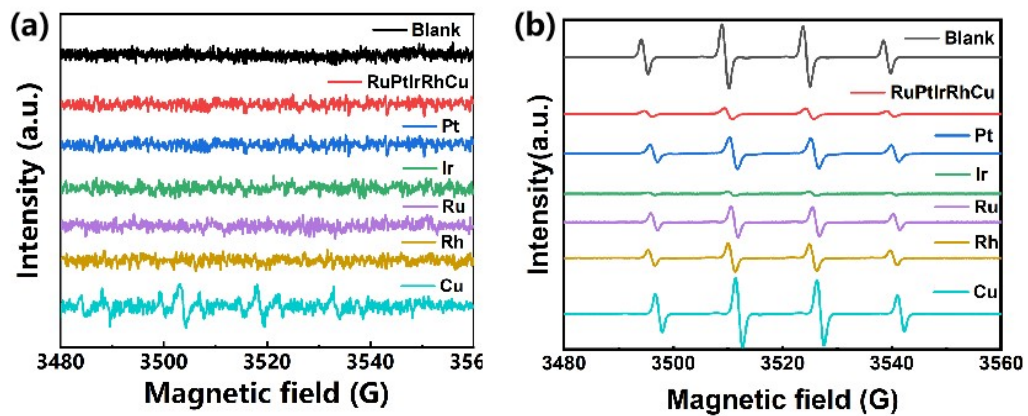


Figure S5. (a) ESR spectra of $\text{H}_2\text{O}_2 + \text{DMPO}$, $\text{H}_2\text{O}_2 + \text{DMPO} + \text{M}$ ($\text{M} = \text{Pt, Ir, Ru, Rh, Cu}$, RuPtIrRhCu HEAzyme). (b) ESR spectra of $\text{Fe}^{2+} \text{H}_2\text{O}_2$, $\text{Fe}^{2+} + \text{H}_2\text{O}_2 + \text{DMPO} + \text{M}$ ($\text{M} = \text{Pt, Ir, Ru, Rh, Cu}$, RuPtIrRhCu HEAzyme).

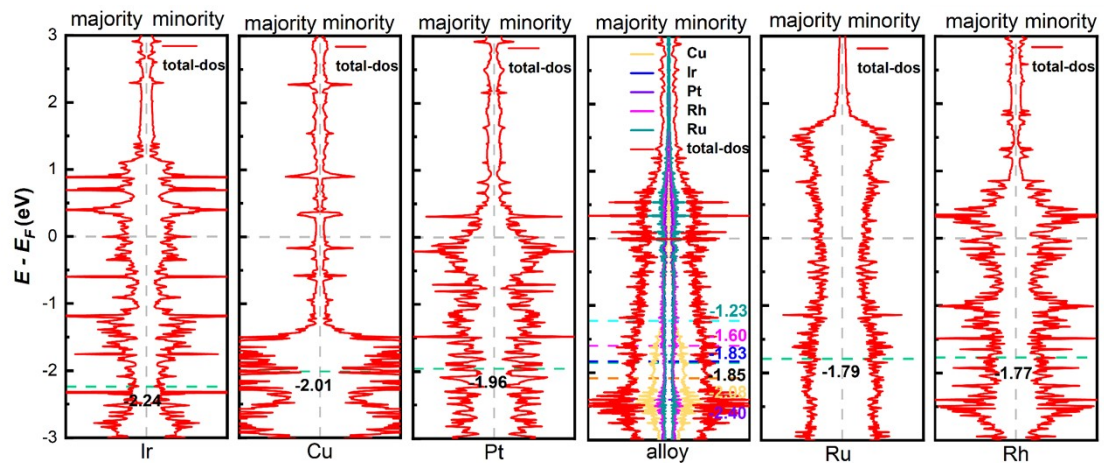


Figure S6. The calculated PDOS for pure metals and their alloy. The dash lines indicate the d-band centers.

Table S1. Structural details of the related materials during calculation.

species	crystal	surface index	supercell	lattice parameters
Rh	fcc ^a	(111)	5×5	$a = b = c = 3.8044, \alpha = \beta = \gamma = 90.0^\circ$
Ir	fcc	(111)	5×5	$a = b = c = 3.8389, \alpha = \beta = \gamma = 90.0^\circ$
Cu	fcc	(111)	5×5	$a = b = c = 3.6147, \alpha = \beta = \gamma = 90.0^\circ$
Ru	hcp ^b	(111)	2×2	$a = b = 2.7058, c = 4.2816,$ $\alpha = \beta = 90.0^\circ, \gamma = 120.0^\circ$
Pt	fcc	(111)	5×5	$a = b = c = 3.9239, \alpha = \beta = \gamma = 90.0^\circ$
alloy	fcc	(111)	5×5	$a = b = c = 3.6147, \alpha = \beta = \gamma = 90.0^\circ$

^a face centered cubic^b hexagonal close-packed

Table S2. Comparison of POD-like kinetic parameters among the nanozymes. V_{\max} represents the reaction activity, and K_m indicates the affinity of the enzyme towards the substrate, respectively. The higher the V_{\max} value, the greater the peroxidase-like activity and the lower the K_m value, the stronger the affinity.

Catalyst	Substrate	K_m (mM)	V_{\max} ($10^{-8} \text{ M}\cdot\text{s}^{-1}$)	Reference
HRP	H_2O_2	3.70	8.71	Lizeng Gao,et al ⁸
	TMB	0.43	10.00	
FeCuAgCeGd	H_2O_2	756	9.65	Sheng Rui et al ⁹
	TMB	6.6	16.9	
PtPdNDs/GNs	H_2O_2	3.45	12.24	Xiaomei Chen ¹⁰
	TMB	0.04	42.67	
Pt@Pd	H_2O_2	4.46	15.7	Mengdie Lei,et al ¹¹
	TMB	0.46	46.3	
AuPtCo	H_2O_2	2.59	10.16	Xiaoyan Zhou,et al ¹²
	TMB	0.14	1.80	
NCFs@PtNi CSSs	H_2O_2	2.58	5.87	Yanwen Mao,et al ¹³
	TMB	1.40	15.7	
Pd-Ir cubes	H_2O_2	340	5.1	Xiaohu Xia,et al ¹⁴
	TMB	0.13	6.5	
PtRuTe	H_2O_2	0.89	26.5	Changshuai Shang,et al ¹⁵
	TMB	0.013	22.30	
PtIrRuRhCu	H_2O_2	0.66	18.33	This work
	TMB	0.017	21.81	

Table S3. Recovery rate of acetylcysteine in the amino acid injection.

Sample	Added (mM)	Measured (mM)	Recovery (%)	RSD (%, n = 3)
1	0.05	0.0584	116.84	
		0.0505	101.07	7.23
		0.0549	109.89	
2	0.1	0.0995	99.46	
		0.1017	101.70	6.62
		0.1124	112.40	
3	0.2	0.1990	103.78	
		0.2143	117.10	8.32
		0.2086	100.21	

Reference

- (1) Grimme, S.; Ehrlich, S.; Goerigk, L., Effect of the damping function in dispersion corrected density functional theory. *J. Comput. Chem.* **2011**, *32* (7), 1456-1465.
- (2) Grimme, S.; Antony, J.; Ehrlich, S.; Krieg, H., A consistent and accurate ab initio parametrization of density functional dispersion correction (DFT-D) for the 94 elements H-Pu. *J. Chem. Phys.* **2010**, *132* (15), 154104.
- (3) Perdew, J. P.; Burke, K.; Ernzerhof, M., Generalized gradient approximation made simple. *Phys. Rev. Lett.* **1996**, *77* (18), 3865.
- (4) Monkhorst, H. J.; Pack, J. D., Special points for Brillouin-zone integrations. *Phys. Rev. B* **1976**, *13* (12), 5188.
- (5) Kresse, G.; Furthmüller, J., Efficiency of ab-initio total energy calculations for metals and semiconductors using a plane-wave basis set. *Comput. Mater. Sci.* **1996**, *6* (1), 15-50.
- (6) Kresse, G.; Joubert, D., From ultrasoft pseudopotentials to the projector augmented-wave method. *Phys. Rev. B* **1999**, *59* (3), 1758.
- (7) Blöchl, P. E., Projector augmented-wave method. *Phys. Rev. B* **1994**, *50* (24), 17953.
- (8) Gao, L.; Zhuang, J.; Nie, L.; Zhang, J.; Zhang, Y.; Gu, N.; Wang, T.; Feng, J.; Yang, D.; Perrett, S.; et al. Intrinsic peroxidase-like activity of ferromagnetic nanoparticles. *Nature Nanotechnology* **2007**, *2* (9), 577-583.
- (9) Sheng, R.; Liu, Y.; Cai, T.; Wang, R.; Yang, G.; Wen, T.; Ning, F.; Peng, H. Ultrafine FeCuAgCeGd-based high-entropy nanozyme: Preparation, catalytic mechanism, and point-of-care detection of dopamine in human serum. *Chemical Engineering Journal* **2024**, *485*, 149913.
- (10) Chen, X.; Su, B.; Cai, Z.; Chen, X.; Oyama, M. PtPd nanodendrites supported on graphene nanosheets: A peroxidase-like catalyst for colorimetric detection of H₂O₂. *Sensors and Actuators B: Chemical* **2014**, *201*, 286-292.
- (11) Lei, M.; Ding, X.; Liu, J.; Tang, Y.; Chen, H.; Zhou, Y.; Zhu, C.; Yan, H. Trace Amount of Bi-Doped Core–Shell Pd@Pt Mesoporous Nanospheres with Specifically

Enhanced Peroxidase-Like Activity Enable Sensitive and Accurate Detection of Acetylcholinesterase and Organophosphorus Nerve Agents. *Analytical Chemistry* **2024**, *96* (15), 6072-6078.

- (12) Zhou, X.; Fan, C.; Tian, Q.; Han, C.; Yin, Z.; Dong, Z.; Bi, S. Trimetallic AuPtCo Nanopolyhedrons with Peroxidase- and Catalase-Like Catalytic Activity for Glow-Type Chemiluminescence Bioanalysis. *Analytical Chemistry* **2022**, *94* (2), 847-855.
- (13) Mao, Y.-W.; Li, J.-Q.; Zhang, R.; Wang, A.-J.; Feng, J.-J. Nitrogen-Doped Carbon Nanoflowers Decorated with PtNi Nanoparticles for Colorimetric Detection of Total Antioxidant Capacity. *ACS Applied Nano Materials* **2023**, *6* (4), 2805-2812.
- (14) Xia, X.; Zhang, J.; Lu, N.; Kim, M. J.; Ghale, K.; Xu, Y.; McKenzie, E.; Liu, J.; Ye, H. Pd–Ir Core–Shell Nanocubes: A Type of Highly Efficient and Versatile Peroxidase Mimic. *ACS Nano* **2015**, *9* (10), 9994-10004.
- (15) Shang, C.; Wang, Q.; Tan, H.; Lu, S.; Wang, S.; Zhang, Q.; Gu, L.; Li, J.; Wang, E.; Guo, S. Defective PtRuTe As Nanozyme with Selectively Enhanced Peroxidase-like Activity. *JACS Au* **2022**, *2* (11), 2453-2459.